FR 82 - 2685

20 International winter meeting on nuclear physics, Bormio (Italy) - 25 - 30 Jan 1982

CEA - CONF -- 6220

LIGHT PARTICLE EMISSION IN LIGHT HEAVY-ION INDUCED REACTIONS

E. Bozek, Y. Cassagnou, R. Dayras, R. Legrain, A. Palmeri[+] and L. Rodriguez
DPh-N/BE, CEN Saclay, 91191 Gif-sur-Yvette Cedex France

and

G. Lanzano, A. Pagano and G. Pappalardo
Ist. Naz. de Fisica Nucleare, Sez. de Catania, 95129 Catania, Italy

[+]On leave of absence from Ist. Naz. de Fisica Nucleare, Sez. de Catania, 95129 Catania, Italy.

1. INTRODUCTION

Limitation to fusion for light systems is still an open question. Recently, in order to try to find an answer to this problem, formation of the compound nucleus ^{26}Al through two different reactions, ^{14}N + ^{12}C and ^{16}O + ^{10}B, has been the object of extensive measurements [1,2] over a large energy region. In the energy range 20 MeV < E_{cm} < 65 MeV, the fusion cross sections for both reactions, shows striking differences (figure 1). Indeed, the fusion cross section for ^{16}O + ^{10}B exceeds that of ^{14}N + ^{12}C by an amount which cannot be simply explained, in the frame of available models, on the basis of calculated or measured nuclear density distributions for these nuclei. A possible explanation for these differences lies in the ability for direct processes to compete more or less efficiently with fusion, according to the nuclei in presence in the entrance channel. In order to verify this hypothesis, we have undertaken a detailed study of the different processes which may compete with fusion in the energy domain where the cross section for fusion deviates from the reaction cross section.

2. EXPERIMENTAL PROCEDURE

Both reactions ^{14}N + ^{12}C and ^{16}O + ^{10}B were used to form the compound nucleus ^{26}Al at the same excitation energy of 44 MeV. From previous fusion cross sections measurements [2], this energy corresponds to the same critical angular momentum $\ell_c \simeq 16\,\hbar$ for both reactions. In the hypothesis of compound nucleus formation, identical mass and charge distributions are expected for the evaporation residues [2].

Self-supporting, $\sim$50 μg/cm^2 thick ^{12}C and ^{10}B targets were bombarded respectively with 62.7 MeV ^{14}N and 63.6 MeV ^{16}O beams produced by the Saclay FN Tandem. Heavy fragments were detected into two telescopes, each consisting of a ΔE gas ionization chamber and a 500-μm surface barrier E-detector. These telescopes with a 1.7° aperture were kept fixed at 10° and 30° relative to the beam direction. Light particles were detected on the other side of the beam into three ΔE(20 μm thick) - E(4 mm thick) solid state telescopes. These telescopes, each with a 3° aperture could be moved from 10° to 170° relative to the beam direction. Single spectra as well as coincidence events between heavy ions and light particles were registered on magnetic tape for off-line analysis.

3. EXPERIMENTAL RESULTS AND DISCUSSION

The experimental results, still preliminary, are qualitatively very similar for both the ^{14}N + ^{12}C and the ^{16}O + ^{10}B reactions and we will consider mainly the

$^{14}N + {}^{12}C$ data.

From the coincidence data, producton of the heaviest residues (Ne, Na and Mg) is consistent with evaporation of light particles from an equilibrated compound nucleus ^{26}Al. However, for lighter residues such as N, O and F, there are evidence for other processes contributing to the yields of these elements. Figure 2 shows a typical two-dimentional plot of the α particle-fluorine coincidences in the $E_\alpha - E_F$ energy plane. Most of the events are concentrated onto two parallel bands as expected from the three-body reaction $^{14}N + {}^{12}C \rightarrow {}^{18}F + 2\alpha$. Events with ^{18}F left in its ground state, should fall on the full curve drawn on figure 2. Spectra of the excitation energy $Q_3 - Q_{3\ g.s.}$ in the final state (which in this particular case is the excitation energy in ^{18}F) are diplayed in figure 3 for three different detection angles of the alpha particle. Most of the events are concentrated into two peaks (corresponding to the two bands of figure 2) centered at 2.32 MeV and 5.34 MeV excitation energy in ^{18}F. An evaporation calculation using the statistical model code CASCADE [3] reproduces quite well the peak at 2.32 MeV but fails to reproduce the peak at 5.34 MeV. This may suggest that this peak does not result from evaporation by the compound nucleus but has its origin in an other mechanism yet to be identified by further analysis of the data.

Figure 4 is a plot of α-nitrogen coincidence events in $E_\alpha - E_N$ energy plane. The full drawn curve is the kinematic locus of events corresponding to the reaction $^{14}N + {}^{12}C \rightarrow {}^{14}N + \alpha + {}^{8}Be$ with ^{14}N and ^{8}Be in their ground state. All events are located inside this curve. A band structure covering the entire energy range of nitrogen fragments is quite visible in the two-dimensional plot of figure 4. This structure decreases in intensity with the α-particle detection angle and have completely disappeared for $\theta_\alpha > 30°$. Such structures are indication of an energy correlation between the α-particles and the nitrogen fragments. Assuming the reaction $^{14}N + {}^{12}C \rightarrow {}^{14}N + \alpha + {}^{8}Be$ the data of figure 4 have been converted into the $Q_3 - Q_{3\ g.s.}$ spectrum of figure 5a. The sharp peak at $Q_3 - Q_{3\ g.s.} = 0$ MeV corresponds to ^{14}N left in its ground state whereas the smaller and broader peak near 2.4 MeV may be associated with the first excited state of ^{14}N. The spectrum of figure 4a has been divided into 5 Q_3 - bins. For each bin, a spectrum of the relative kinetic energy E_r of the α and the ^{14}N in their center-of-mass system has been built and converted into a spectrum of excitation energy in ^{18}F. Well defined peaks are clearly seen for gates 1,4 and 5. The presence of such peaks is hardly conceivable in the frame of statistical evaporation and are more likely due to a reaction of the type $^{14}N + {}^{12}C \rightarrow {}^{18}F^* + {}^{8}Be$ and $^{18}F^* \rightarrow {}^{14}N + \alpha$. In the contrary for gates 2 and 3, the excitation energy spectra are dominated by a continuum which is consistent with statistical evaporation. The two processes cannot be separated by a simple examination of ^{14}N energy spectra, and in inclusive measurements, they are usually included in the fusion cross section.

At our bombarding energies, fusion does not contribute to the yields of boron and carbon fragments which are mainly produced through direct reactions. Energy correlations between light particles and these fragments are essentially consistent with three-body final states as illustrated in figure 6. In the Q_3 - spectrum of figure 6a, corresponding to the reaction $^{14}N + {}^{12}C \rightarrow {}^{10}B + \alpha + {}^{12}C$, only two three-body final states are seen : one corresponding to ^{10}B and ^{12}C left in their ground state and the other corresponding to ^{12}C left in its first excited state. The Q_3 - spectrum associated with the reactions $^{14}N + {}^{12}C \rightarrow {}^{13}C + p + {}^{12}C$ and $^{14}N + {}^{12}C \rightarrow {}^{12}C + d + {}^{12}C$ are shown in figure 6b. There again only few final states are seen. The relative energy spectra for $^{10}B - \alpha$, $^{13}C - p$ and $^{12}C - d$ of figure 7 have been obtained by selecting events corresponding to the ground state Q_3 - peak in each case. The strong peak in the relative kinetic energy spectrum of $^{10}B - \alpha$ corresponds to an excitation energy of $\sim$ 12.8 MeV ^{14}N and is probably the same state observed by Pr. Siemssen (this Conference and ref. [4]) in the sequential decay of ^{14}N in the reaction $^{14}N + {}^{159}Tb$ at much higher energy. Similarly the peaks observed in the relative kinetic energy spectra of $^{13}C - p$ and $^{12}C - d$ can be related to excited states or groups of excited states in ^{14}N. Thus break-up of the projectile seems to proceed through the excitation of well defined states in ^{14}N followed by sequential decay.

3. CONCLUSIONS

The transition between fusion and direct processes is not as clear cut as it is usually assumed and so-called evaporation residues may include a non-negligible contributions from other processes. However a more quantitative analysis remains to be done to derive more quantitative results.

At our bombarding energy (4.5 MeV/A), break-up of the projectile proceeds essentially though excitation of well defined states in the projectile followed by sequential decay.

REFERENCES

[1] J. Gomez del Campo, R.G. Stokstad, J.A. Biggerstaff, R.A. Dayras, A.H. Snell, and P.H. Stelson, Phys. Rev. C19 (1979) 2170.

[2] J. Gomez del Campo, R.A. Dayras, J.A. Biggerstaff, D. Shapira, A.H. Snell, P.H. Stelson and R.G. Stokstad, Phys. Rev. Lett. 43 (1979) 26.

[3] F. Pühlhofer, Nucl. Phys. A280 (1977) 267.

[4] J. Van Driel, S. Gonggrijp, R.V.F. Janssens, R.H. Siemssen, K. Siwek-Wilczynska and J. Wilczynski, Phys. Lett. 98B (1981) 351.

FIGURE CAPTIONS

Fig. 1 : Fusion cross sections vs $1/E_{cm}$ for $^{14}N + ^{12}C$ and $^{16}O + ^{10}B$ (ref. [2]).

Fig. 2 : Two-dimensional plot of α-F coincidence events. The full drawn curve is the kinematic locus for events corresponding to the three-body reaction $^{14}N + ^{12}C \rightarrow ^{18}F + 2\alpha$ with ^{18}F in its ground state.

Fig. 3 : Q_3 - spectra for the reaction $^{14}N + ^{12}C \rightarrow ^{18}F + 2\alpha$. Note that the ground state $Q_{3\ g.s.}$ value = - 11.6 MeV has been subtracted from Q_3 before plotting. Thus the abscissa represent excitation energy in ^{18}F.

Fig. 4 : Two-dimensional plot of α-N coincidence events. The full drawn curve represents the kinematic locus for events corresponding to the three-body reaction $^{14}N + ^{12}C \rightarrow ^{14}N + \alpha + ^{8}Be$ with ^{14}N left in its ground state. The band structure, clearly visible is discussed in the text.

Fig. 5 : a) Q_3-spectrum assuming the reaction $^{14}N + ^{12}C \rightarrow ^{14}N + \alpha + ^{8}Be$. The ground state $Q_{3\ g.s.}$ value = - 7.37 MeV has been subtracted before plotting. b-f) Excitation energy spectra in ^{18}F for different gates on the Q_3-spectrum.

Fig. 6 : - Q_3 - spectra for the reactions $^{14}N + ^{12}C \rightarrow ^{10}B + \alpha$ (a) and $^{14}N + ^{12}C \rightarrow ^{13}C + p + ^{12}C$ and $^{14}N + ^{12}C \rightarrow ^{12}C + d + ^{12}C$ (b). The heavy fragments and the light particles were detected at ± 10° relative to the beam direction.

Fig. 7 : Relative energy spectra for a) ^{10}B-α, b) ^{13}C-p and c) ^{12}C-d. Only events corresponding to ground state Q_3 - values have been selected. The geometry is that of figure 6.

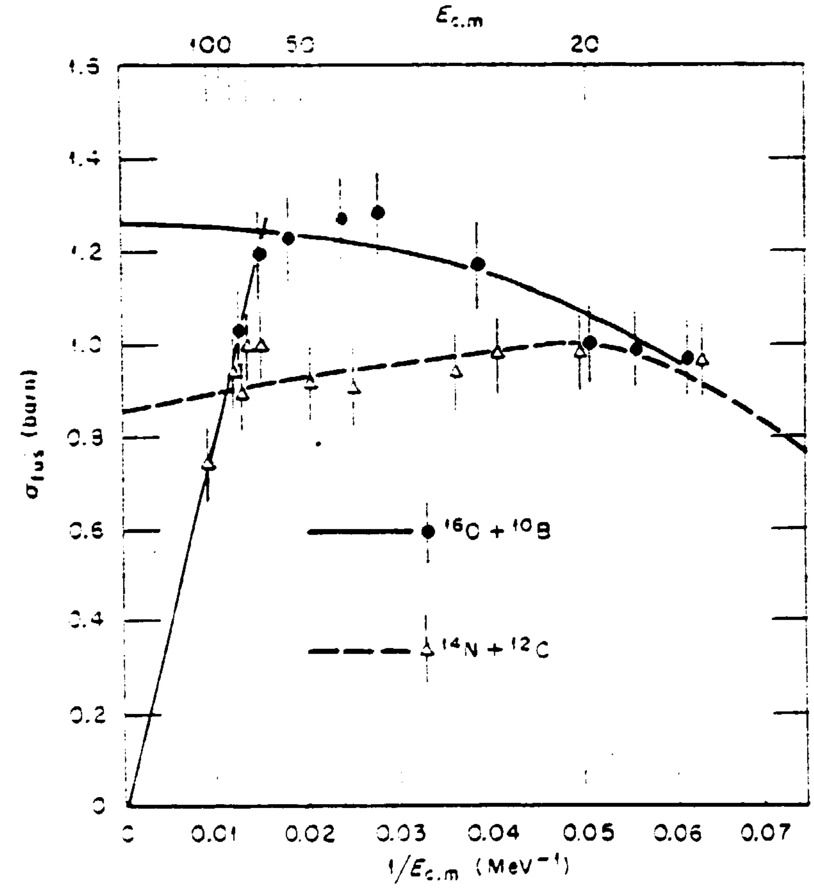

$E_{c.m}$
100
50
20
1.6
1.4
1.2
1.0
0.8
0.6
0.4
0.2
0
σ_{fus} (barn)
$^{16}O + ^{10}B$
$^{14}N + ^{12}C$
0
0.01
0.02
0.03
0.04
0.05
0.06
0.07
$1/E_{c.m}$ (MeV^{-1})

Fig. 1

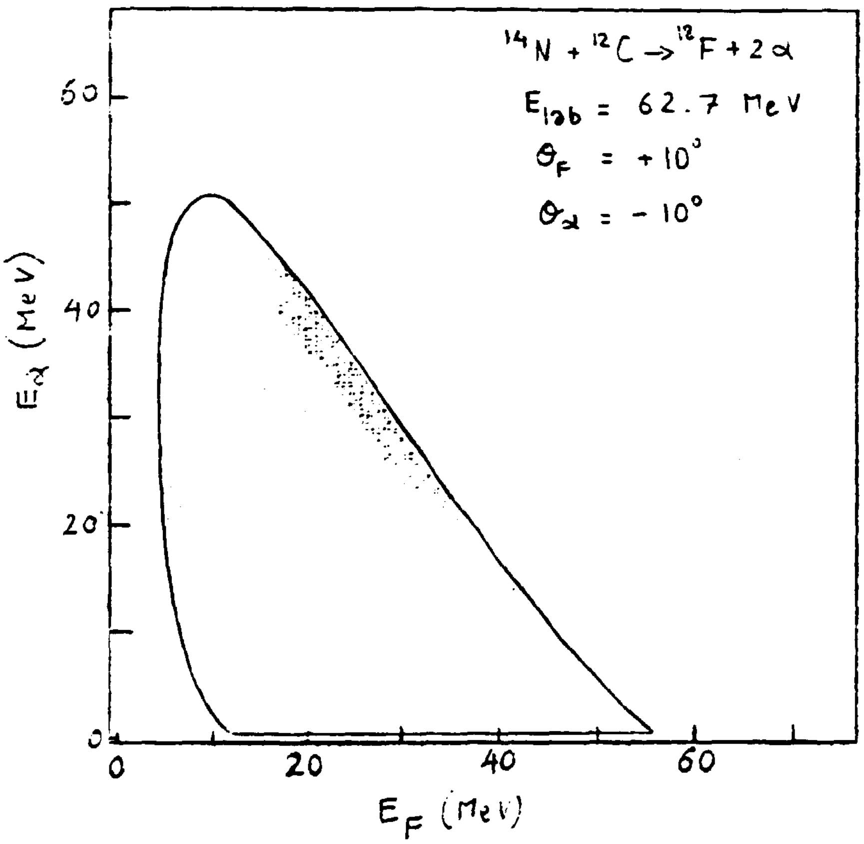

$^{14}N + ^{12}C \rightarrow ^{12}F + 2\alpha$
E_{lab} = 62.7 MeV
θ_F = +10°
θ_α = -10°
60
40
20
0
20
40
60
E_α (MeV)
E_F (MeV)

Fig. 2

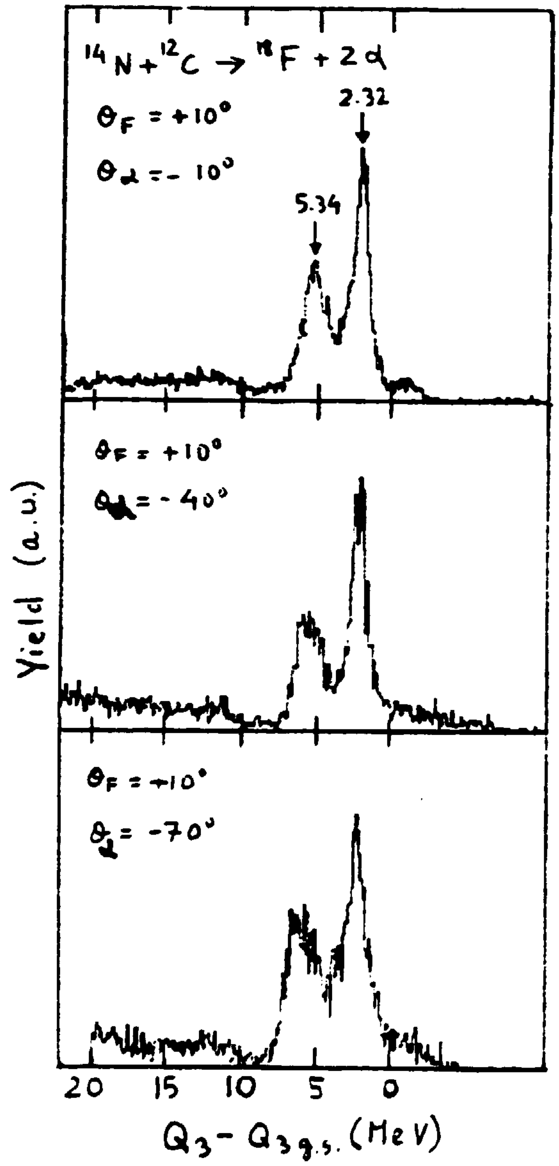
$^{14}N+^{12}C \rightarrow ^{18}F+2\alpha$
$\theta_F = +10°$
$\theta_\alpha = -10°$
2.32
5.34
$\theta_F = +10°$
$\theta_\alpha = -40°$
$\theta_F = +10°$
$\theta_\alpha = -70°$
Yield (a.u.)
20 15 10 5 0
$Q_3 - Q_{3g.s.}$ (MeV)

Fig. 3

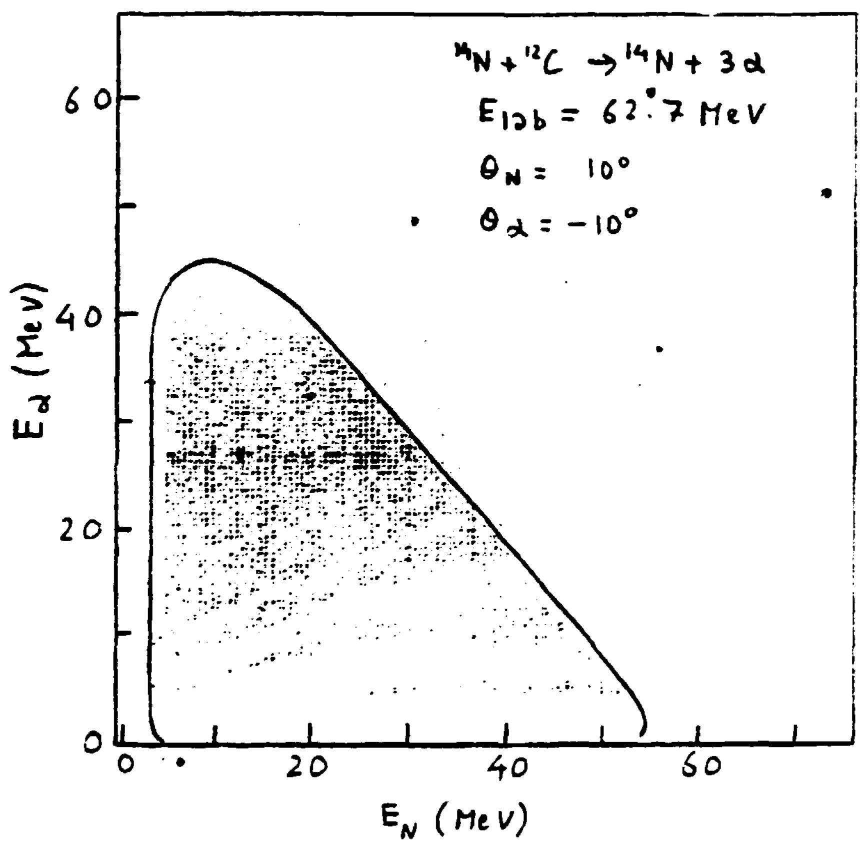

$^{14}N + ^{12}C \rightarrow ^{14}N + 3\alpha$
E_{lab} = 62.7 MeV
θ_N = 10°
θ_α = −10°
60
40
20
0
0
20
40
60
E_α (MeV)
E_N (MeV)

Fig. 4

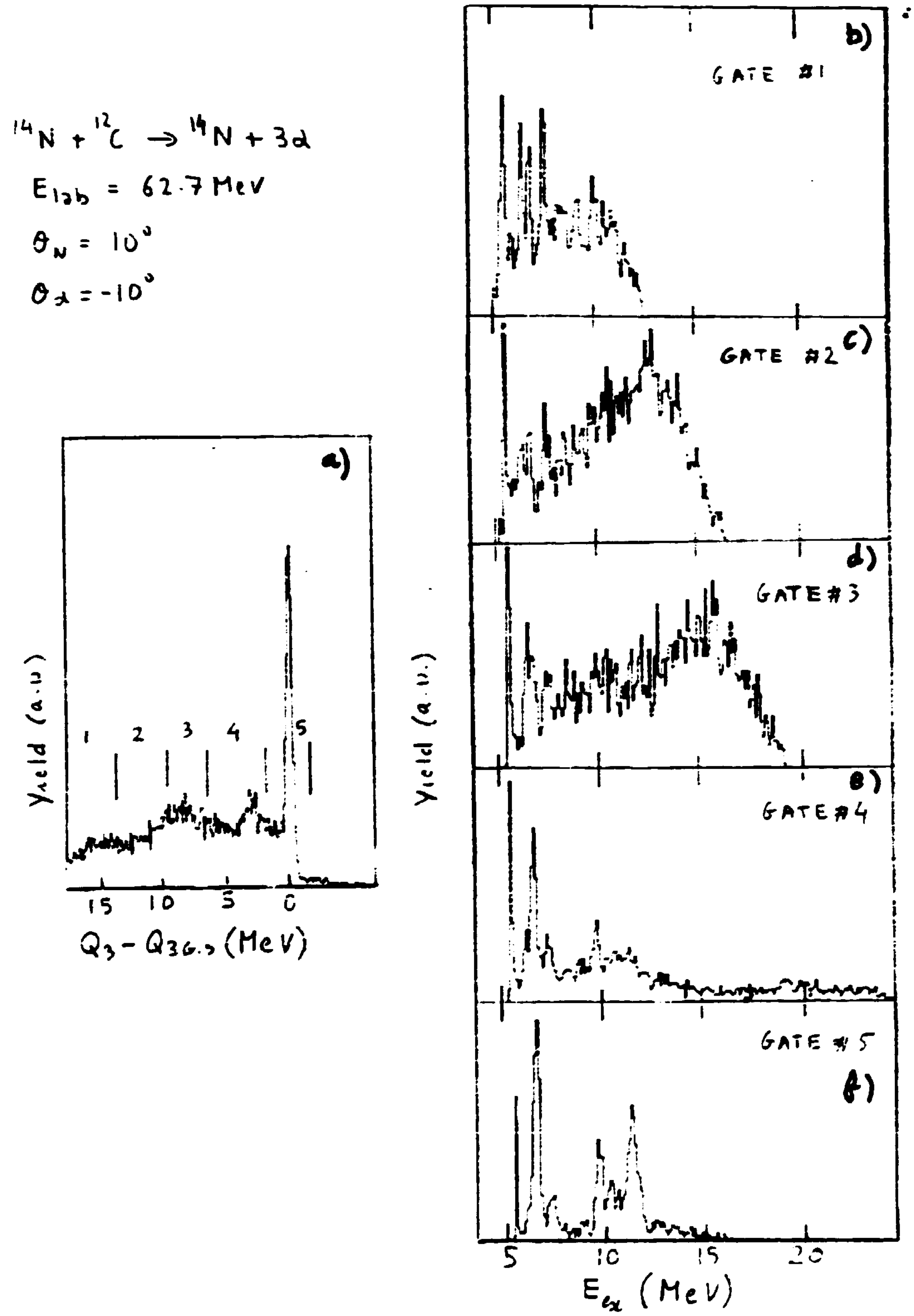
14N + 12C → 14N + 3α
Elab = 62.7 MeV
θN = 10°
θα = -10°
a)
1
2
3
4
5
15
10
5
0
Q3 - Q36.5 (MeV)
Yield (a.u.)
b)
GATE #1
GATE #2
c)
d)
GATE#3
e)
GATE#4
GATE #5
f)
5
10
15
20
Eex (MeV)
Yield (a.u.)

Fig. 5

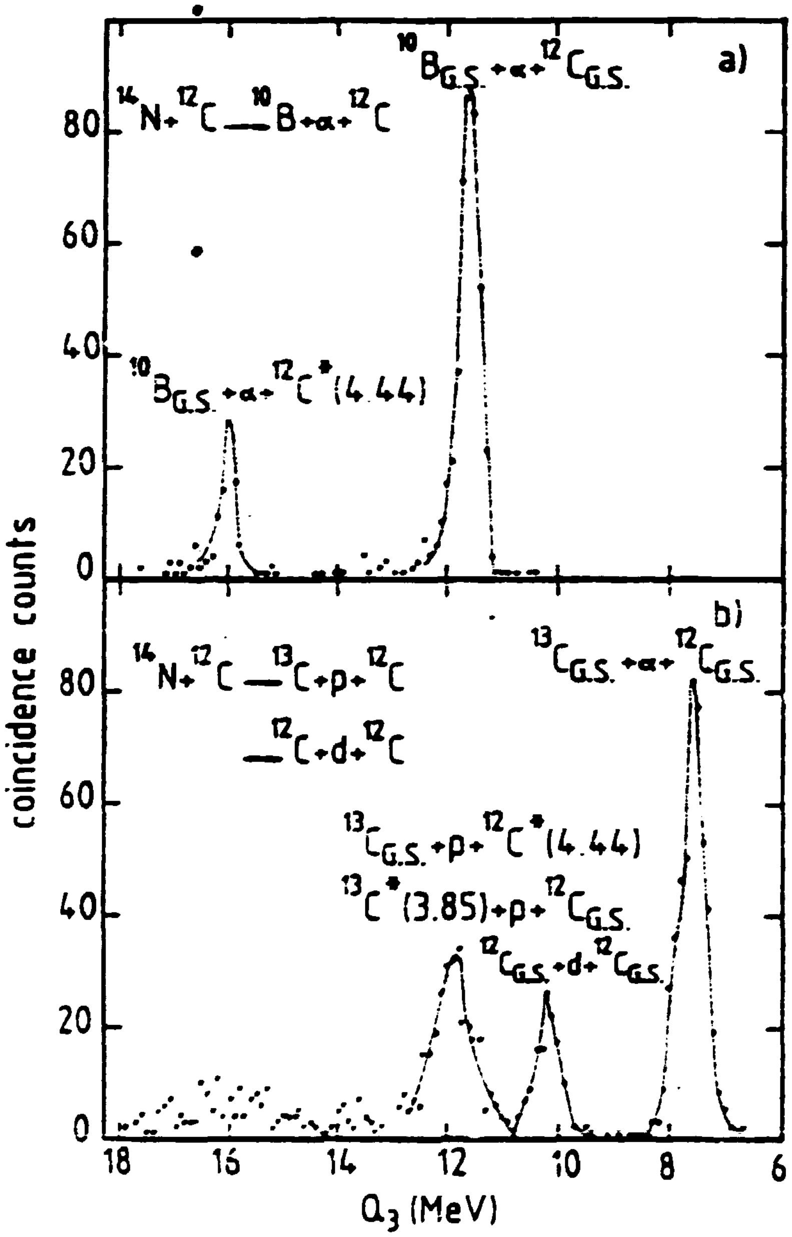

a)
14N+12C — 10B+α+12C
10B G.S.+α+12C G.S.
10B G.S.+α+12C*(4.44)
b)
14N+12C — 13C+p+12C
— 12C+d+12C
13C G.S.+α+12C G.S.
13C G.S.+p+12C*(4.44)
13C*(3.85)+p+12C G.S.
12C G.S.+d+12C G.S.
coincidence counts
Q3 (MeV)
0
20
40
60
80
18
16
14
12
10
8
6

Fig. 6

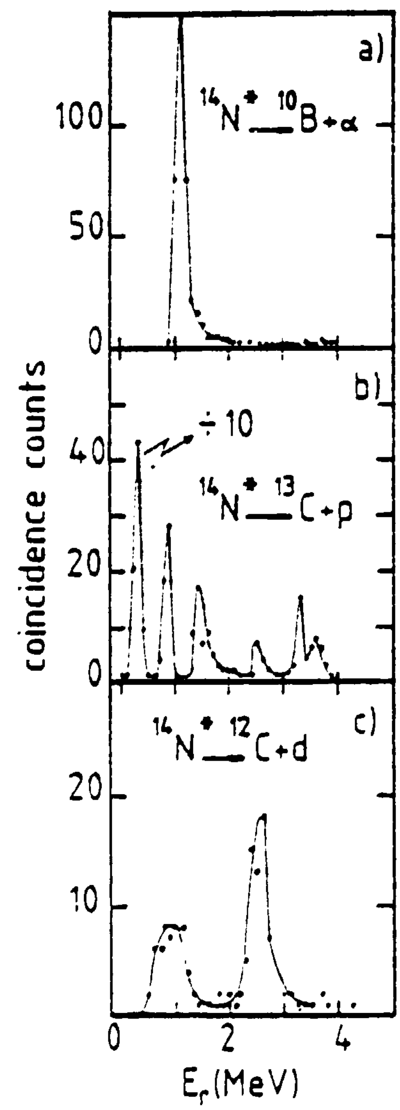
a)
$^{14}N^* \longrightarrow {}^{10}B+\alpha$
b)
÷ 10
$^{14}N^* \longrightarrow {}^{13}C+p$
c)
$^{14}N^* \longrightarrow {}^{12}C+d$
coincidence counts
100
50
0
40
20
0
20
10
0
2
4
E_r(MeV)

Fig. 7